ORIGINAL ARTICLE
(CC BY-SA)
UDC: 618.19-006-08:547.9
DOI: https://doi.org/10.2298/VSP260701060A

Identification of a plant-derived terpenoid as a potential TET1 modulator in breast cancer

Identifikacija terpenoida biljnog porekla kao potencijalnog modulatora TET1 u karcinomu dojke

[1]Ahmed M. Alharbi*, [1]Pratibha Pandey[†], Asmatanzeem Bepari[‡], Rasha Assad Assiri[§], Danah A. Alturbak[‖], Mohd Saeed[¶], Meenakshi Verma[†], Shivani Sharma, Fahad Khan[††]**

University of Hail, *College of Applied Medical Sciences, Department of Medical Laboratory Science, [¶]College of Science, Department of Biology, Hail, Saudi Arabia; [†]Chandigarh University, University Center for Research and Development, Mohali, Punjab, India; Princess Nourah bint Abdulrahman University, College of Medicine, [‡]Department of Basic Sciences, [§]Department of Basic Medical Sciences, Riyadh, Saudi Arabia; [‖]King Saud University, College of Applied Medical Sciences, Department of Clinical Laboratory Sciences, Riyadh, Saudi Arabia; **Uttaranchal University, Uttaranchal Institute of Technology, Dehradun, Uttarakhand, India; [††]Saveetha Institute of Medical and Technical Sciences, Saveetha Medical College and Hospitals, Department of Community Medicine, Chennai, India

[1]**equal contribution of both authors**

Abstract

Background/Aim. Breast cancer progression is driven by dysregulated signaling pathways and epigenetic alterations. Plant-derived terpenoids have attracted significant attention as promising anticancer agents due to their ability to modulate key molecular and cellular targets. Ten-eleven translocation 1 (TET1) has been identified as an oncogenic factor in aggressive breast cancer subtypes, promoting tumor-supporting transcriptional activities at specific DNA sites and contributing to resistance against oxidative stress-mediated cell death. The aim of this study was to examine the potential of plant-derived terpenoids to target TET1 and to explore the correlation between TET1 modulation, oxidative stress, and apoptosis-mediated cell death in breast carcinoma. **Methods.** Molecular docking using a curvature-based docking approach and *in vitro* assessment of the effects of cryptotanshinone on cell viability, reactive oxygen species (ROS) generation, apoptosis, and the mRNA expression levels of *TET1, SLC7A11*, and *GPX4* in MCF-7 cells were performed to investigate the anticancer potential of plant-derived terpenoids mediated by modulation of TET1 activity in breast cancer. **Results.** A high binding affinity of cryptotanshinone for the CXXC domain of TET1 was found, along with favorable drug-like properties, and cryptotanshinone was selected as the potent terpenoid for further analysis. *In vitro* evaluation revealed a dose-dependent reduction in cell viability of cryptotanshinone-treated MCF-7 cells and apoptotic induction. Additionally, gene expression analysis showed decrease in the mRNA levels of *TET1*, *SLC7A11*, and *GPX4* in a dose-dependent manner, suggesting alterations in antioxidant defense pathway signaling. **Conclusion.** Cryptotanshinone may exert anticancer effects associated with apoptosis induction and oxidative stress modulation, potentially involving the epigenetic regulator TET1, in breast cancer cells. Further studies using animal models and clinical samples are necessary to confirm the therapeutic potential of cryptotanshinone in the treatment of breast cancer.

Keywords:
apoptosis; breast neoplasms; computer simulation; gene expression; in vitro; plant extracts; terpenes.

Apstrakt

Uvod/Cilj. Progresija karcinoma dojke podstaknuta je disregulacijom signalnih puteva i epigenetskim promenama. Terpenoidi biljnog porekla privukli su značajnu pažnju kao potencijalni antikancerogeni agensi zbog svoje sposobnosti da modulišu ključne molekularne i ćelijske mete. *Ten-eleven translocation 1* (TET1) identifikovan je kao onkogeni faktor u agresivnim podtipovima karcinoma dojke, koji podstiče transkripcione aktivnosti na

Correspondence to: Fahad Khan, Saveetha Institute of Medical and Technical Sciences, Saveetha Medical College and Hospitals, Department of Community Medicine, Chennai, India. E-mail: fahadintegralian@gmail.com

specifičnim mestima DNK koje doprinose razvoju tumora i otpornosti na ćelijsku smrt posredovanu oksidativnim stresom. Cilj rada bio je da se ispita potencijal terpenoida biljnog porekla da ciljano deluje na TET1, kao i da se ispita povezanost između modulacije TET1, oksidativnog stresa i apoptozom-indukovane ćelijske smrti u karcinomu dojke. **Metode.** Za ispitivanje antitumorskog potencijala terpenoida biljnog porekla posredovanog modulacijom aktivnosti TET1 u karcinomu dojke primenjeni su molekulsko dokovanje metodom *curvature-based docking* i *in vitro* procena efekata kriptotanšinona na vijabilnost ćelija, stvaranje reaktivnih kiseoničnih vrsta *(reactive oxygen species* – ROS), apoptozu i nivoe ekspresije iRNK gena *TET1, SLC7A11* i *GPX4* u ćelijama MCF-7. **Rezultati.** Utvrđen je visok afinitet vezivanja kriptotanšinona za CXXC domen TET1, uz povoljne osobine slične svojstvima lekova, pa je kriptotanšinon odabran kao potentni terpenoid za dalju analizu. *In vitro* procena pokazala je dozno-zavisno smanjenje vijabilnosti MCF-7 ćelija tretiranih kriptotanšinonom, kao i indukciju apoptoze. Pored toga, analiza ekspresije gena pokazala je dozno-zavisno smanjenje nivoa iRNK gena *TET1*, *SLC7A11* i *GPX4*, što ukazuje na promene u signalnim putevima antioksidativne odbrane. **Zaključak.** Kriptotanšinon može ispoljiti antikancerogeno delovanje povezano sa indukcijom apoptoze i modulacijom oksidativnog stresa, uz moguću uključenost epigenetskog regulatora TET1, u ćelijama karcinoma dojke. Neophodna su dalja istraživanja na životinjskim modelima i kliničkim uzorcima kako bi se potvrdio terapijski potencijal kriptotanšinona u lečenju karcinoma dojke.

Ključne reči:
ćelija, smrt; dojka, neoplazme; simulacija, kompjuterska; geni, ekspresija; in vitro; ekstrakti, biljni; terpeni.

Introduction

Breast cancer is still one of the most frequently diagnosed cancers and ranks as a leading cause of cancer-related mortality among women across the globe. Although there are significant advancements in targeted therapeutic approaches, including early detection, several issues, such as recurrence leading to treatment failure, pose major challenges in triple-negative breast cancer [1]. Several factors are largely responsible for therapy resistance, metastasis, and the capability of tumor cells to adapt to oxidative and metabolic stress [2]. Thus, identifying new molecular targets that can circumvent resistance mechanisms and trigger non-apoptotic tumor cell death is essential [3]. Epigenetic dysregulation has been recognized as a fundamental feature of breast carcinoma, promoting abnormal gene expression patterns that lead to cell proliferation, invasion, and immune evasion. Among all potent epigenetic regulators, ten-eleven translocation 1 (TET1) is known to influence transcriptional activation at cytosine-phosphate-guanine (CpG)-rich genomic regions by oxidizing 5-methylcytosine [4]. Increasing evidence suggests that TET1 may function as an oncogenic driver in breast carcinoma by enhancing metastatic, stemness, and epithelial-mesenchymal transition efficacy through locus-specific epigenetic modifications; however, these effects are context- and isoform-dependent [5, 6]. Targeting the catalytic domain of TET1 remains challenging because of limited structural data and potential inadvertent effects on global deoxyribonucleic acid (DNA) methylation dynamics. TET1 has a conserved CXXC zinc-finger DNA-binding domain that facilitates its interaction with CpG islands and regulatory promoters, thereby enabling transcriptional regulation without enzymatic activity. Therefore, targeting TET1-DNA interactions offers strong potential that further adds to the field of structure-based drug design. In contrast to traditional catalytic inhibitors, focusing on the DNA-binding interface may enhance locus specificity, hence obstructing TET1-mediated activation of oncogenic transcriptional networks at the chromatin level [7, 8].

In apoptosis-resistant breast carcinoma, ferroptosis has attracted increasing attention by inducing reactive oxygen species (ROS) production and lipid accumulation [9]. Two upregulated antioxidant defense systems–nuclear factor erythroid 2-related factor 2 (NRF2)-mediated redox homeostasis and the solute carrier family 7 member 11 (SLC7A11)/glutathione peroxidase 4 (GPX4) axis–mainly help tumor cells to avoid ferroptosis [10]. According to recent research, TET1 (an epigenetic regulator) may be associated with cancer-linked signaling pathways and redox homeostasis through maintaining transcriptional activity [11]. Therefore, molecular docking-based targeting of the TET1 CXXC DNA-binding domain could be a novel epigenetic strategy to explore the TET1-mediated anticancer mechanisms in breast cancer. We focus on the CXXC domain of full-length TET1 ($TET1^{FL}$) not because it drives the phosphoinositide 3-kinase (PI3K)-associated oncogenic activity attributed to the CXXC-lacking isoform of TET1 ($TET1^{ALT}$) [6], but because $TET1^{FL}$-CXXC-mediated CpG binding governs a distinct transcriptional axis relevant to tumor cell survival: locus-specific demethylation that may sustain expression of antioxidant defense genes such as *SLC7A11* and GPX4. We hypothesize that disrupting this CXXC-DNA interaction could reduce antioxidant gene expression and increase oxidative-stress vulnerability in breast cancer cells, representing a mechanism of therapeutic relevance distinct from, and narrower than, $TET1^{ALT}$-driven proliferative oncogenesis. Small compounds found through docking may interact with the TET1 CXXC DNA-binding domain and influence TET1-linked transcriptional programs of antioxidant networks and redox homeostasis [12].

Therefore, the aim of this study was to utilize a molecular docking-based screening of terpenoids against the TET1 CXXC DNA-binding domain, followed by *in vitro* evaluation of the lead compound for its anticancer activity and TET1-associated molecular responses in breast cancer Michigan Cancer Foundation-7 (MCF-7) cells.

Methods

Software used for in silico investigation

Structural retrieval of the target protein was done using the Protein Data Bank (PDB), and ligand acquisition was done using the PubChem server available online. Additionally, the Curvature-based dock (CB-Dock) server was utilized for performing blind docking and cavity prediction. It uses the AutoDock Vina engine to estimate binding affinity and PyMOL visualizer to visualize the binding interactions.

Chemicals and Reagents

Dulbecco's Modified Eagle's Medium (DMEM) (AT151), fetal bovine serum (FBS) (RM10434), and antibiotic-antimycotic solution (A002) were procured from HiMedia Laboratories Pvt. Ltd., Mumbai, India. All supplementary analytical-grade chemicals and reagents used in this research were acquired from reputable commercial vendors and possessed the highest purity. Cryptotanshinone [C5624-5mg, ≥ 98% high-performance liquid chromatography (HPLC) grade], methyl thiazolyl tetrazolium (MTT) (M2128, 98%, powder), and 2',7'-dichlorodihydrofluorescein diacetate (DCFH-DA) (D6883, ≥ 97% HPLC) were procured from Sigma-Aldrich, St. Louis, MO, USA, and stock solutions were developed in dimethyl sulfoxide (DMSO) and stored at -20 °C for future usage. The final DMSO concentration was kept below 0.1% (v/v) through meticulous dilution of the working concentrations in the growth medium. Invitrogen SuperScript™ III One-Step reverse transcription PCR (RT-PCR) System (Cat. No. 12574018) was purchased from Thermo Fisher Scientific, while Annexin V fluorescein isothiocyanate (FITC)-conjugated Apoptosis Detection Kit I BD Pharmingen™ (Cat. No. 556547) was purchased from BD Biosciences, San Jose, CA, USA.

Protein and ligand preparation for molecular docking

Three-dimensional (3D) crystal structure of the human TET1 CXXC DNA-binding domain (PDB ID: 6ASD) was selected due to its significance in CpG recognition and experimental resolution. CXXC domain of $TET1^{FL}$ was targeted not only because it drives the PI3K-associated oncogenic activity attributed to the CXXC-lacking $TET1^{ALT}$ isoform, but also because $TET1^{FL}$-CXXC-mediated CpG binding governs a distinct transcriptional axis critical to tumor cell survival: locus-specific demethylation that may sustain expression of antioxidant defense genes such as *SLC7A11* and *GPX4*. Before docking, the protein was stripped of co-crystallized DNA, water molecules, and non-ligand-binding heteroatoms. Missing residues were examined, and hydrogen atoms were added to ensure structural integrity. The protein structure was saved as a PDB file for docking analysis. The PubChem database provided the chemical structures of the selected ligands. Ligands were energy-minimized to obtain stable conformations and were preserved in SDF or MOL2 format. The improved ligand files were then translated to the docking submission format.

Molecular docking using CB-Dock

CB-Dock integrates curvature-based cavity detection with AutoDock Vina-based blind docking to automatically identify potential binding cavities and predict protein–ligand binding poses [13]. The CB-Dock server received the receptor protein (TET1 CXXC domain, PDB: 6ASD). Ligand structures were uploaded individually in the SDF/MOL2 format. Due to curvature-based pocket recognition, CB-Dock found protein binding cavities automatically. The server generated numerous binding cavities sorted by cavity volume and docking capability for each ligand. AutoDock Vina docking simulations produced binding poses and affinity scores (kcal/mol) [14].

The docking output comprised top-ranked binding cavities, projected binding energies, ligand-protein interaction poses, 3D and 2D interaction representations, docking scores, and interaction analyses. Docking results were assessed by binding affinity scores and ligand orientation stability in the anticipated binding pocket. Low binding energy and favorable molecular interactions determined the optimal docking conformations. PyMOL and Discovery Studio Visualizer were used to study protein-ligand interactions, such as hydrogen bonding, hydrophobic contacts, and electrostatic interactions. Residues important for CpG recognition within the CXXC DNA-binding interface were prioritized, as their disruption may prevent TET1 recruitment to genomic targets. Thus, docking to the TET1 CXXC domain provides structural insights into small molecules that modulate TET1-DNA interactions. Modulation of epigenetically regulated antioxidant pathways may increase oxidative stress sensitivity in breast cancer cells, informing the development of novel oxidative stress-inducing therapies.

Pharmacokinetic suitability of the selected ligands using SwissADME

Within the context of the current in silico investigation of antioxidant-pathway-associated proteins in breast cancer, the pharmacokinetic and drug-likeness profiles of the selected ligands were further evaluated using the SwissADME web tool [15]. Particular attention was paid to the gastrointestinal (GI) absorption, bioavailability score [16], and drug-likeness properties. These attributes reflect the ability of the ligand to enter systemic circulation and cross the intestinal barrier and help determine the efficacy of oral drugs. In addition, the bioavailability score is a crucial prognostic indicator of the likelihood that a molecule will display acceptable oral exposure. It does this by incorporating critical physicochemical characteristics such as molecular size, polarity, and lipophilicity of the molecule. Furthermore, the evaluation of drug-likeness through the use of known filters, such as Lipinski's rule of five [17], guarantees that promising candidates for oxidative stress-modulating properties contain advantageous structural and pharmacological qualities that go

beyond docking affinity alone. Collectively, these factors increase the translational relevance of the compounds identified by supporting their potential as orally viable therapeutic agents for managing breast cancer through modulation of oxidative stress pathways.

Assessment of cell viability and half-maximal inhibitory concentration

We obtained the MCF-7 breast cancer cell line from the National Center for Cell Science, Pune, India. The cancer cells were cultured in DMEM containing 10% FBS (Himedia India, Mumbai, India) and 1% antibiotic-antimycotic solution (Himedia India, Mumbai, India). We maintained optimal cell growth conditions in an incubator at 37 °C with 5% carbon dioxide – CO_2. The effect of cryptotanshinone on the cell viability of breast carcinoma MCF-7 cells was assessed using the MTT assay. MCF-7 cells (6,000 cells/well) were plated in 96-well plates and then exposed to different doses of cryptotanshinone (0–8 μM) for 24 hrs. After 24 hrs, 10 μL of MTT dye was transferred to the treated wells, which were then left for 2 hrs at 37 °C. The formazan crystal was then dissolved with 100 μL DMSO, and the microplate reader (Bio-Rad, USA) was used to calculate the optical density.

Furthermore, the half-maximal inhibitory concentration (IC_{50}) value of cryptotanshinone was calculated using GraphPad Prism software (GraphPad Prism Software Inc., San Diego, CA, USA). A dose-response parameter with nonlinear regression was selected to obtain the response curve. The percentage of cell viability was plotted against the logarithm of the cryptotanshinone dose and IC_{50} values were derived from the fitted sigmoidal curve. This method facilitates the selection of concentrations from sub-cytotoxic to cytotoxic levels, thereby minimizing non-specific cell death. The selection of lower concentrations maintains sufficient cell viability to evaluate early molecular and biochemical changes, such as ROS generation and apoptosis induction. Medium-range concentrations facilitate the identification of gradual signaling changes and initiation of apoptotic pathways. At the same time, doses above IC_{50} create an environment favorable for observing significant apoptotic responses without total reduction in viable cells.

Assessment of reactive oxygen species generation

Effects of cryptotanshinone on ROS-mediated oxidative stress were determined using DCFH-DA labelling, as previously outlined by Alshammari et al. [18]. In short, 1×10^4 MCF-7 cells were treated with cryptotanshinone at three different concentrations (2, 4, and 6 μM) for 12 hrs. Cells were later treated with DCFH-DA (10 mM) at 37 °C for 30 min. Then, the intensity of the fluorescence was measured using a multiwell microplate reader (Synergy H1 Hybrid Multi-Mode Microplate Reader, BioTek, USA). To further confirm the cryptotanshinone's efficacy in ROS generation, cells were previously treated with a ROS inhibitor, 10 mM N-acetyl-L-cysteine (NAC), for 2 hrs. The same methods of ROS analysis were then carried out as previously described.

Quantitative real-time polymerase chain reaction analysis

The total ribonucleic acid (RNA) of cryptotanshinone-treated MCF-7 cells was collected and used to convert into complementary DNA – cDNA using a reverse transcription kit. Relative messenger RNA (mRNA) expression of the TET1 transcript region and antioxidant defense-related molecular targets following cryptotanshinone exposure were evaluated by quantitative real-time polymerase chain reaction (PCR) – qPCR. Relative mRNA expression levels were normalized to β-actin as the internal reference gene. For each sample, the difference between the cycle threshold (Ct) value of the target gene and that of β-actin was calculated as ΔCt, where: [ΔCt = Ct(target gene) - Ct(β-actin)]. The normalized expression level was calculated as ($2^{-\Delta Ct}$). Relative changes in target gene expression between treated and control samples were subsequently determined using the ($2^{-\Delta\Delta Ct}$) method, where: [ΔΔCt= ΔCt(treated)-ΔCt(control)], and relative fold expression was calculated as ($2^{-\Delta\Delta Ct}$). The control group was used as the calibrator and assigned a relative expression value of 1.0. Ct denotes the cycle threshold at which the fluorescence signal crosses the defined detection threshold. Primer sequences are listed in Table 1.

Flow cytometric analysis of apoptosis

To assess apoptosis, Annexin V Apoptosis Detection Kit I (BD Pharmingen™, BD Biosciences, San Jose, CA, USA; Cat. No. 556547) was used according to the manufacturer's instructions. MCF-7 cells (1 × 106 cells/well) were seeded and exposed to different concentrations of cryptotanshinone (2, 4, and 6 μM) after 24 hrs, whereas control cells were maintained under identical conditions without treatment. Breast cancer cells were mixed with 100 μL of binding buffer containing propidium iodide (PI) (5 μg/mL) and annexin V-FITC (0.125 μg/mL). They were then

Table 1

Primer sequences used for quantitative real-time PCR analysis

Gene	Forward primer	Reverse primer
TET1	5'-TCTGTTGTTGTGCCTCTGGA-3'	5'-GCCTTTAAAACTTTGGGCTTC-3'
GPX4	5'-GCCTTTGCCGCCTACTGAAG-3'	5'-ACGAAGCCCCGGTACTTGTC-3'
SLC7A11	5'-GCTCCATGAACGGTGGTGTG-3'	5'-AGAGGAGTGTGCTTGCGGAC-3'
β-actin	5'-GTCTGTGATGCCCTTAGATG-3'	5'-AGCTTATGACCCGCACTTAC-3'

PCR – polymerase chain reaction; *TET1* – ten-eleven translocation 1; *GPX4* – glutathione peroxidase 4; *SLC7A11* – solute carrier family 7 member 11.

incubated at room temperature in the dark for 15 min. We analyzed the samples using a flow cytometer (BD FACSCaliburTM Flow Cytometer; BD Biosciences, San Diego, CA, USA) to determine the proportion of early and late apoptotic cells relative to the remaining cells.

Statistical analysis

The mean ± standard error of the mean is used to represent all datasets of three independent experiments (n = 3). One-way analysis of variance – ANOVA was selected to calculate the results, and the GraphPad Prism tool was employed to conduct Dunnett's multiple comparison test. Data statistical significance was determined by a probability *p*-value less than 0.05.

Results

Drug-likeness and pharmacokinetic profiles of selected terpenoids

Parameters were selected to assess the potential of plant-based compounds as potent candidates for developing anticancer agents. Although numerous parameters exist, we selected only Lipinski criteria, GI absorption, and Bioavailability score for our study. These parameters are essential pharmacokinetic factors that are used in anticancer drug development to assess the oral bioavailability and therapeutic potential of candidate compounds. Lipinski's parameters are utilized for identifying compounds with favorable permeability, solubility, and overall drug-likeness. In cancer therapeutics, GI tract absorption reflects how much of an orally administered drug reaches systemic circulation and influences therapeutic efficacy, formulation strategy, and toxicity. In addition to GI and Lipinski parameters, the bioavailability score provides an approximate proportion of the selected drug that remains unaltered in systemic circulation, which is required for dose optimization, systemic toxicity minimization, and reduced treatment failure. These selected parameters form a fundamental framework for the rational design, screening, and optimization of orally active plant-based products, thereby increasing the likelihood of anticancer therapeutic approaches. The cryptotanshinone compound has shown better outcomes than all other selected terpenoids (Table 2).

Molecular docking and binding affinity analysis of selected terpenoids

Docking was done to elucidate the potent terpenoid that has displayed the best inhibitory activity against the TET1 target. In Table 3, it can be clearly seen that cryptotanshinone has shown the best binding efficacy (-7.0) in docking analysis in comparison to all other selected compounds. Thus, in further sections, we performed two *in vitro* methods, including MTT and RT-PCR assays, to investigate the efficacy of cryptotanshinone in breast carcinoma.

Effect of cryptotanshinone on MCF-7 cell viability

Treatment of MCF-7 cells with cryptotanshinone at concentrations of 0.5, 1, 2, 4, and 8 μM reduced cell viability to 82.74 ± 4.72% ($p < 0.05$), 64.78 ± 4.12% ($p < 0.05$), 55.45 ± 4.33% ($p < 0.001$), 42.9 ± 3.91% ($p < 0.001$), and 23.68 ± 3.53% ($p < 0.001$), respectively, compared with the control sample. In Figure 1A, it can be seen that cryptotanshinone has shown maximum inhibitory potential at its highest dose (8 μM). Based on the dose-response curve, the IC_{50} was 3.89 ± 0.93 μM (Figure 1B). This IC_{50} value was further used to select the doses needed for ROS generation and RT-PCR analysis.

Table 2

Predicted drug-likeness and pharmacokinetic properties of selected plant-derived terpenoids

Compound	Compound identifier	Chemical formulae	Lipinski's rule of five	Gastrointestinal absorption	Bioavailability score
Arnicolide D	182199	$C_{19}H_{24}O_5$	yes; 0 violation	high	0.55
Cryptotanshinone	160254	$C_{19}H_{20}O_3$	yes; 0 violation	high	0.85
Glycyrrhetinic acid	10114	$C_{30}H_{46}O_4$	yes; 1 violation: MLogP > 4.15	high	0.85
Eupaformosanin	5281453	$C_{22}H_{28}O_8$	yes; 0 violation	high	0.55
Artemisinin	68827	$C_{15}H_{22}O_5$	yes; 0 violation	high	0.55
Dihydroartemisinine	3000518	$C_{15}H_{24}O_5$	yes; 0 violation	high	0.55
Tanshinone IIA	164676	$C_{19}H_{18}O_3$	yes; 0 violation	high	0.55
Oridonin	5321010	$C_{20}H_{28}O_6$	yes; 0 violation	high	0.55

MLogP – Moriguchi Log P.

Table 3

Docking results showing Vina scores, interacting residues, and protein–ligand interactions

Compound	Vina scores	Contact residues	Protein-ligand interaction
Arnicolide D	-6.0	chain C: LYS587 ARG588 LYS589 ARG590 CYS597 ASN602 TYR608 CYS609 ARG612 SER615 HIS616 GLN617 ILE618 CYS619 ARG622 LYS623 CYS624 LEU627	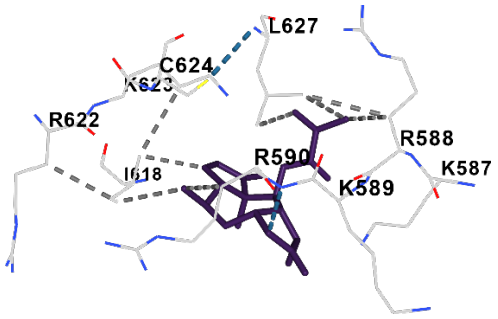
Cryptotanshinone	-7.0	chain C: LYS587 ARG588 LYS589 ARG590 THR607 TYR608 ASN611 ASN614 SER615 HIS616 GLN617 ILE618 CYS619 LYS620 LYS623 LEU627 LYS628 LYS629 LYS630	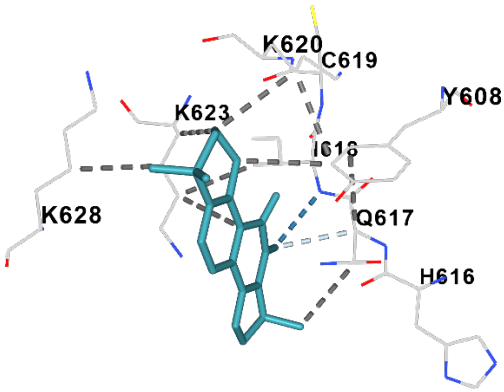
Glycyrrhetinic acid	-6.6	chain C: LYS587 ARG588 LYS589 ARG590 ASN602 TYR608 CYS609 ARG612 LYS613 SER615 HIS616 GLN617 ILE618 CYS619 ARG622 LYS623 CYS624 LEU627	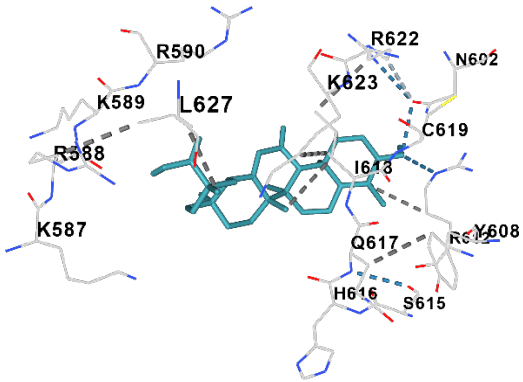
Eupaformosanin	-5.7	chain C: GLY586 LYS587 ARG588 LYS589 ARG590 PRO596 CYS597 TYR608 HIS616 GLN617 ILE618 CYS619 LYS620 LYS621 ARG622 LYS623 CYS624 GLU625 LEU627 LYS628 LYS629 LYS630	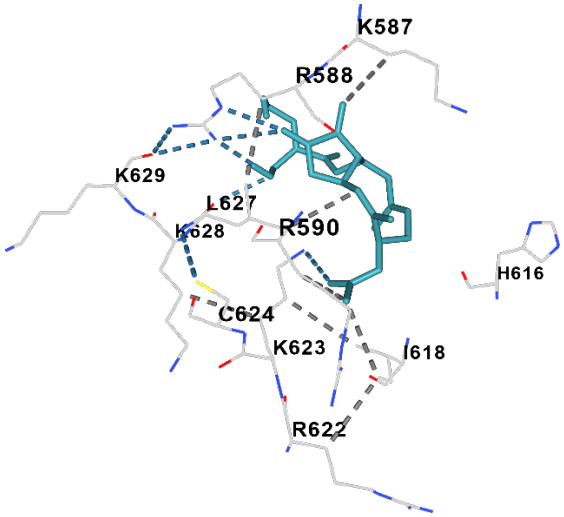

Table 3 (continued)

Compound	Vina scores	Contact residues	Protein-ligand interaction
Artemisinin	-6.2	chain C: TYR608 GLN617 ILE618 CYS619 LYS620 LYS623 LEU627 LYS628	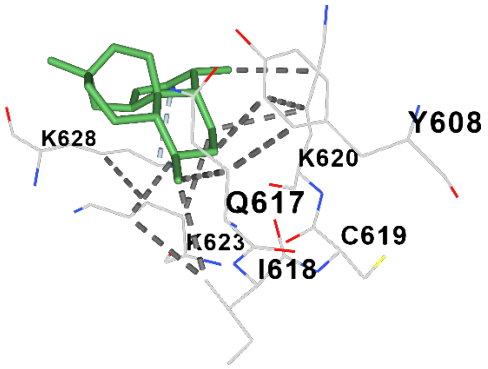
Dihydroartemisinine	-5.9	chain C: TYR608 GLN617 ILE618 CYS619 LYS620 LYS623 LEU627 LYS628	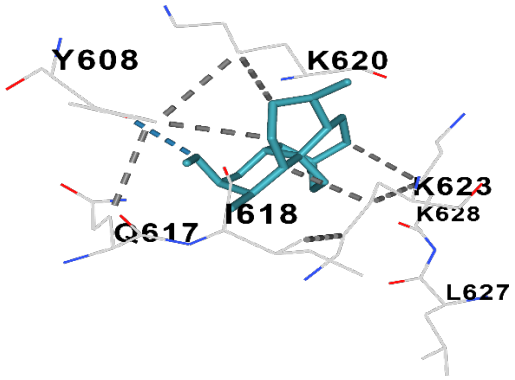
Tanshinone IIA	-6.7	chain C: GLY586 LYS587 ARG588 TYR608 HIS616 GLN617 ILE618 CYS619 LYS620 LYS623 LEU627 LYS628	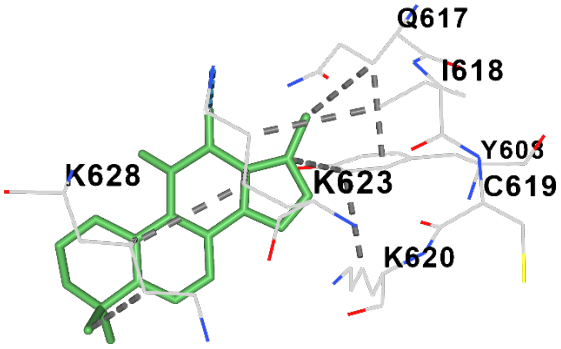
Oridonin	-6.3	chain C: TYR608 GLN617 ILE618 CYS619 LYS620 LYS621 LYS623 LEU627 LYS628	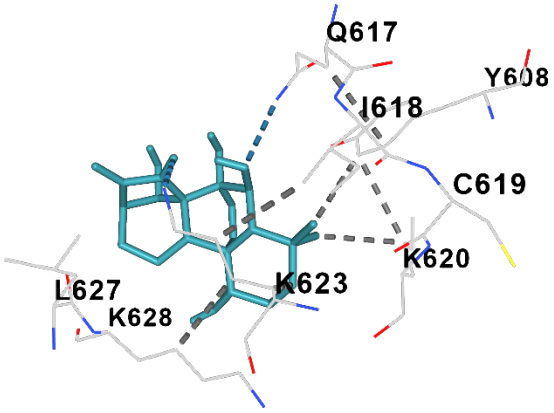

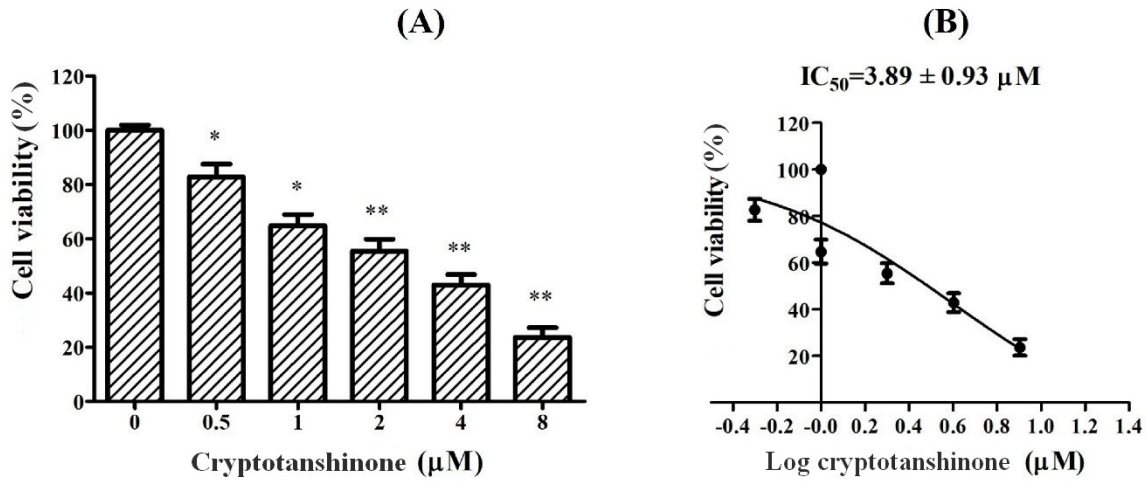

Fig. 1 – A) MTT result showing cell viability inhibition in cryptotanshinone-treated MCF-7 cells; B) dose-dependent IC_{50} curve of cryptotanshinone.
Data are represented as mean ± standard error of the mean of three independent experiments (n = 3).
***Note*: *$p < 0.05$; **$p < 0.001$ compared with the control sample.**
IC_{50} – half-maximal inhibitory concentration; MTT – methyl thiazolyl tetrazolium; MCF-7 – Michigan Cancer Foundation-7; n – number.

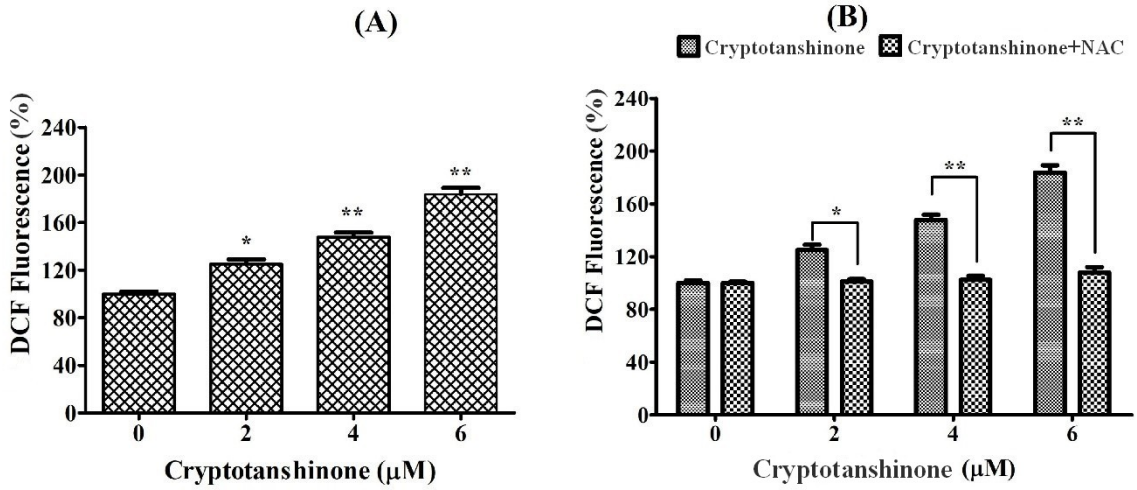

Fig. 2 – Cryptotanshinone induced ROS generation in breast cancer MCF-7 cells: A) effect of cryptotanshinone (0, 2, 4, and 6 μM) on ROS generation in MCF-7 cells; B) quenching of ROS in NAC pre-treated MCF-7 cells.
Data are represented as mean ± standard error of the mean of three independent experiments (n = 3).
***Note*: *$p < 0.05$, **$p < 0.001$ compared with the control sample.**
DCF – dichlorodihydrofluorescein; NAC – N-acetyl-L-cysteine; ROS – reactive oxygen species; MCF-7 – Michigan Cancer Foundation-7; n – number.

Cryptotanshinone-induced reactive oxygen species generation in MCF-7 cells

ROS generation was markedly elevated in a concentration-dependent manner following treatment with 2, 4, and 6 μM doses of cryptotanshinone to approximately 24.96 ± 4.08% ($p < 0.05$), 47.11 ± 3.93% ($p < 0.001$), and 83.78 ± 5.33% ($p < 0.001$), respectively, compared with the control sample (Figure 2A). When the cells were pretreated with the ROS inhibitor NAC and subsequently exposed to cryptotanshinone, the results clearly showed reduced ROS levels in MCF-7 cells (Figure 2B). Based on these results, ROS production might play a role in the cryptotanshinone-induced cell viability inhibition in breast cancer MCF-7 cells.

Effect of cryptotanshinone on TET1, SLC7A11, and GPX4 mRNA expression

To analyze the effects of cryptotanshinone on mRNA expression of *TET1* and associated genes (*SLC7A11* and

GPX4), we performed RT-PCR analysis. As shown in Figure 3, cryptotanshinone significantly downregulated *TET1* mRNA levels to 0.67 ± 0.071 ($p < 0.001$), 0.35 ± 0.049 ($p < 0.001$), and 0.21 ± 0.026 ($p < 0.001$), alongside the *SLC7A11* mRNA expression to 0.82 ± 0.081 ($p < 0.05$), 0.49 ± 0.077 ($p < 0.001$), and 0.24 ± 0.057 ($p < 0.001$), and *GPX4* mRNA expression to 0.77 ± 0.085 ($p < 0.05$), 0.47 ± 0.04 ($p < 0.001$), and 0.29 ± 0.026 ($p < 0.001$) at 2, 4, and 6 μM concentrations, respectively, compared with the control sample.

Cryptotanshinone-induced apoptosis in MCF-7 cells

It was explored whether cryptotanshinone induced apoptosis in MCF-7 cells. Annexin V/PI double staining method showed that the apoptosis rate was markedly increased to 12.6 ± 1.29% ($p < 0.05$), 21.6 ± 2.88% ($p < 0.001$), and 34.2 ± 2.63% ($p < 0.001$), respectively, following a 24 hrs exposure to cryptotanshinone at different concentrations of 2, 4, and 6 μM (Figure 4).

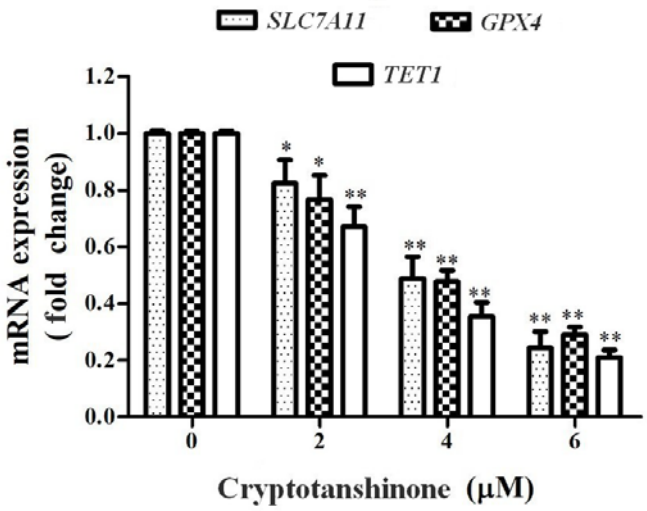

Fig. 3 – RT-PCR analysis for investigating mRNA expression in cryptotanshinone-treated MCF-7 cells.
Data are represented as mean ± standard error of the mean of three independent experiments (n = 3).
***Note*: *$p < 0.05$; **$p < 0.001$ compared with control sample.**
mRNA – messenger ribonucleic acid; *SLC7A11* – solute carrier family 7 member 11; *TET1* – ten-eleven translocation 1; *GPX4* – glutathione peroxidase 4; RT-PCR – reverse transcription polymerase chain reaction; MCF-7 – Michigan Cancer Foundation-7; n – number.

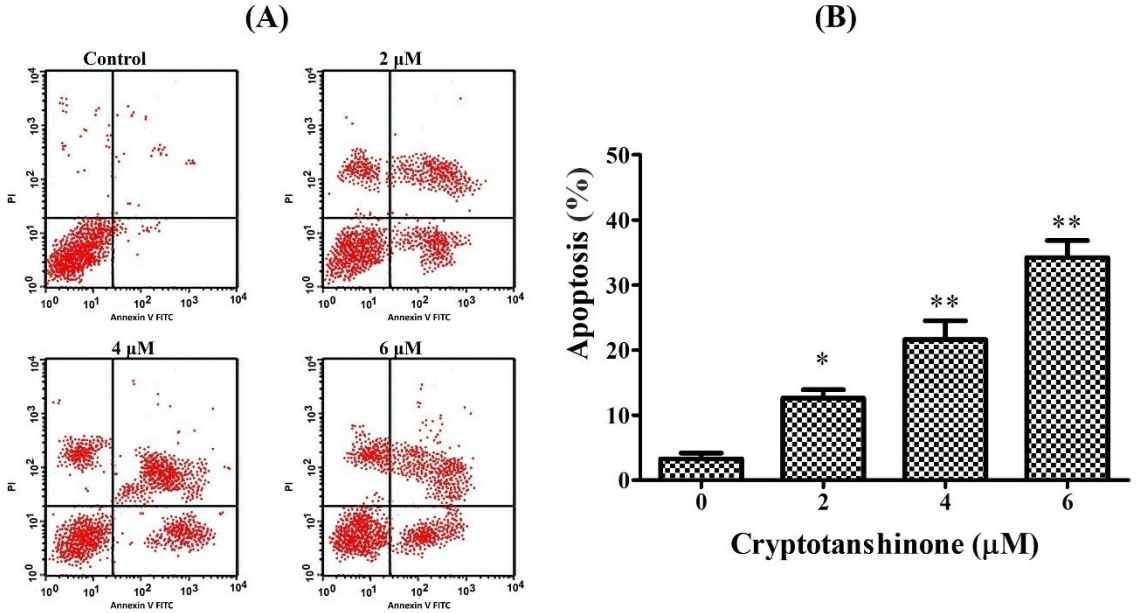

Fig. 4 – Cryptotanshinone-induced apoptosis in breast cancer MCF-7 cells: A) the percent apoptotic cells treated with different concentrations of cryptotanshinone (0, 2, 4, and 6 μM) for 24 hrs analyzed by flow cytometry; B) percentage of apoptotic cells increased following exposure to cryptotanshinone compared with the untreated control.
Data are represented as mean ± standard error of the mean of three independent experiments (n = 3).
***Note*: *$p < 0.05$; **$p < 0.001$ compared with the control sample.**
PI – propidium iodide; FITC – fluorescein isothiocyanate; MCF-7 – Michigan Cancer Foundation-7; n – number.

Discussion

TET1 is an epigenetic regulator often linked to the development of breast cancer because of its involvement in oncogenic pathway transcriptional activation and DNA demethylation [19]. The DNA-binding CXXC domain of TET1 is similarly important because it controls locus-specific recruitment to CpG-rich promoters and enhancers, even though most research focuses on the catalytic dioxygenase activity of TET1 proteins [20]. Abnormal TET1 activity in breast cancer increases tumor formation, metastasis, epithelial-mesenchymal transition, and treatment resistance by activating genes linked to invasion and stemness [21]. Previous studies showed that blocking the DNA-binding domain of TET1 provided a novel means of limiting its function upstream, thereby preventing its localization to oncogenic target regions, even in the absence of direct enzymatic activity inhibition [22–24]. Importantly, TET1-mediated epigenetic reprogramming (genome-wide) leads to disruption of the DNA-binding interface that blocks transcriptional networks associated with aggressive triple-negative breast cancer. Because it offers selective epigenetic intervention and broadens anti-TET1 drug development beyond catalytic inhibitors, targeting the DNA-binding domain is a promising therapeutic approach [25].

Docking with the CXXC DNA-binding domain is crucial since it investigates the disruption of protein-DNA interactions, an emerging technique in anticancer research. TET1 is recognized as an epigenetic regulator that associates with CpG-rich genomic regions *via* its CXXC domain, thereby facilitating the transcriptional activation of genes involved in redox balance, lipid metabolism, and cellular survival [26, 27]. Growing data demonstrate that abnormal TET1-mediated epigenetic reconfiguration may influence cellular redox homeostasis by modulating antioxidant defense pathways, including SLC7A11 and GPX4 [11, 28].

Inhibiting CXXC-mediated DNA binding may prevent locus-specific demethylation processes that sustain tumor cell adaptation to oxidative damage [29]. Thus, docking-based discovery of small compounds that can interfere with the TET1-DNA binding interface may improve oxidative stress-mediated response in aggressive breast cancer subtypes. This epigenetic drug discovery technique targets redox homeostasis, which may help overcome drug resistance and metastasis. Ferroptosis investigations often target GPX4 inhibitors or system xc− inhibition [30], while targeting the epigenetically associated target TET1 may provide a novel strategy for exploring the modulation of these pathways [31].

Among the selected terpenoids, cryptotanshinone showed the best binding interaction with TET1 using CB-Dock analysis. MCF-7 cells treated with cryptotanshinone have shown significant inhibition of cell viability of MCF-7 cells. Moreover, the findings from the Annexin V-FITC assay demonstrated that cryptotanshinone exposure markedly increased apoptotic cell populations in a dose-dependent fashion, consistent with a previous study [32]. Additionally, RT-PCR analysis showed that cryptotanshinone-mediated *TET1* inhibition resulted in enhanced suppression of *SLC7A11* and *GPX4* in breast cancer MCF-7 cells. Our results are in accordance with a study that demonstrated the inhibitory effects of longikaurin A on TET2 expression, accompanied by GPX4 downregulation and ferroptosis induction in glioblastoma [33]. Altogether, this preliminary study suggests that TET1 may be involved in the anticancer effects of cryptotanshinone through mechanisms associated with oxidative stress and apoptosis in MCF-7 breast cancer cells. This potential involvement is supported by molecular docking results and changes in *TET1*, *SLC7A11*, and *GPX4* mRNA expression, together with increased ROS generation and apoptosis following cryptotanshinone treatment. However, further experimental validation, including TET1 protein expression analysis and *in vivo* studies, is required to clarify the role of TET1 in the anticancer effects of cryptotanshinone. Additionally, isoform-specific expression profiling and locus-specific chromatin analyses are warranted to further investigate the proposed molecular mechanisms.

Conclusion

This study showed that cryptotanshinone has the strongest binding affinity for TET1 CXXC DNA-binding domain. *In vitro* experiments demonstrated that cryptotanshinone reduced MCF-7 cell viability, increased reactive oxygen species generation, and induced apoptosis in a concentration-dependent manner. Furthermore, cryptotanshinone treatment downregulated the mRNA expression of *TET1*, *SLC7A11*, and *GPX4*, suggesting a potential association between its cytotoxic effects and alterations in oxidative stress-related pathways. Although these findings support the potential anticancer activity of cryptotanshinone in breast cancer cells, the underlying molecular mechanisms, particularly the involvement of TET1, require further investigation. Additional studies using animal models and clinical samples are needed to validate these findings and assess the therapeutic potential of cryptotanshinone in breast cancer.

Acknowledgement and funding

This work was supported by Princess Nourah bint Abdulrahman University Researchers Supporting Project (PNURSP2026R148), Princess Nourah bint Abdulrahman University, Riyadh, Saudi Arabia.

Conflict of interest

The authors declare no conflict of interest.

R E F E R E N C E S

1. *Tang DD, Ye ZJ, Liu WW, Wu J, Tan JY, Zhang Y,* et al. Survival feature and trend of female breast cancer: A comprehensive review of survival analysis from cancer registration data. Breast 2025; 79: 103862. DOI: 10.1016/j.breast.2024.103862.
2. *Jeong W, Lee SJ*. Engineering Complexity: Advances in 3D Breast Cancer Models for Precision Oncology. Adv Healthc Mater 2026; 15(1): e03104. DOI: 10.1002/adhm.202503104.
3. *Song J, Yang P, Chen C, Ding W, Tillement O, Bai H,* et al. Targeting epigenetic regulators as a promising avenue to overcome cancer therapy resistance. Sig Transduct Target Ther 2025; 10(1): 219. DOI: 10.1038/s41392-025-02266-z.
4. *Yu Y, Qi J, Xiong J, Jiang L, Cui D, He J,* et al. Epigenetic Co-Deregulation of EZH2/TET1 is a Senescence-Countering, Actionable Vulnerability in Triple-Negative Breast Cancer. Theranostics 2019; 9(3): 761–77. DOI: 10.7150/thno.29520.
5. *Wu X, Zhang Y*. TET-mediated active DNA demethylation: mechanism, function and beyond. Nat Rev Genet 2017; 18(9): 517–34. DOI: 10.1038/nrg.2017.33.
6. *Good CR, Panjarian S, Kelly AD, Madzo J, Patel B, Jelinek J,* et al. TET1-Mediated Hypomethylation Activates Oncogenic Signaling in Triple-Negative Breast Cancer. Cancer Res 2018; 78(15): 4126–37. DOI: 10.1158/0008-5472.CAN-17-2082.
7. *Dunican DS, Pennings S, Meehan RR*. The CXXC-TET bridge — mind the methylation gap! Cell Res 2013; 23(8): 973–4. DOI: 10.1038/cr.2013.71.
8. *Yang S, Li X, Bao L, Cui J, Liu J, Cong S,* et al. Evolutionary and structural insights into DNMTs and TETs: decoding their functional heterogeneity and oncogenic roles in methylation regulation. BMC Mol and Cell Biol 2025; 26(1): 26. DOI: 10.1186/s12860-025-00552-w.
9. *Zhang K, Guo L, Li X, Hu Y, Luo N*. Cancer-associated fibroblasts promote doxorubicin resistance in triple-negative breast cancer through enhancing ZFP64 histone lactylation to regulate ferroptosis. J Transl Med 2025; 23(1): 247. DOI: 10.1186/s12967-025-06246-3.
10. *Zhao S, Zheng M, Ma G, Niu K, Zhang L*. An integrated analysis of SLC7A11 as a pan-cancer immunotherapeutic biomarker with experimental validation of its regulation by miR-148b-3p in breast cancer. Front Immunol 2026; 17: 1752767. DOI: 10.3389/fimmu.2026.1752767.
11. *Yang L, Lu J, Yun W, Yang X, Sun J, Ge C,* et al. TET1 as a master regulator controlling GPX4-dependent and -independent ferroptosis surveillance in acute myeloid leukemia. Nat Commun 2026; 17(1): 1800. DOI: 10.1038/s41467-026-68509-x.
12. *Pandey P, Mallick MdN, Ali S, Verma M, Lakhanpal S, Sharma S,* et al. Emerging role of plant-based compounds as ferroptosis modulators in breast cancer. Naunyn-Schmiedeberg's Arch Pharmacol 2026; 1–8. DOI: 10.1007/s00210-026-05602-4.
13. *Liu Y, Grimm M, Dai WT, Hou MC, Xiao ZX, Cao Y*. CB-Dock: a web server for cavity detection-guided protein–ligand blind docking. Acta Pharmacol Sin 2020; 41(1): 138–44. DOI: 10.1038/s41401-019-0228-6.
14. *Trott O, Olson AJ*. AutoDock Vina: Improving the speed and accuracy of docking with a new scoring function, efficient optimization, and multithreading. J Comput Chem 2010; 31(2): 455–61. DOI: 10.1002/jcc.21334.
15. *Daina A, Michielin O, Zoete V*. SwissADME: a free web tool to evaluate pharmacokinetics, drug-likeness and medicinal chemistry friendliness of small molecules. Sci Rep 2017; 7(1): 42717. DOI: 10.1038/srep42717.
16. *Martin YC*. A Bioavailability Score. J Med Chem 2005; 48(9): 3164–70. DOI: 10.1021/jm0492002.
17. *Lipinski CA, Lombardo F, Dominy BW, Feeney PJ*. Experimental and computational approaches to estimate solubility and permeability in drug discovery and development settings. Adv Drug Deliv Rev 2001; 46(1–3): 3–26. DOI: 10.1016/s0169-409x(00)00129-0.
18. *Alshammari N, Pandey P, Redhwan A, Bakhsh HR, Lakhanpal S, Rab SO,* et al. Unraveling the Ferroptosis-inducing Potential of Methanol Leaves Extract of Prosopis Juliflora Via Downregulation of SLC7A11 and GPX4 mRNA Expression in A549 Lung Cancer Cells. Curr Med Chem 2025; 32(7): 1442–56. DOI: 10.2174/0109298673343133241011072425.
19. *Bao B, Teslow EA, Mitrea C, Boerner JL, Dyson G, Bollig-Fischer A*. Role of TET1 and 5hmC in an Obesity-Linked Pathway Driving Cancer Stem Cells in Triple-Negative Breast Cancer. Mol Cancer Res 2020; 18(12): 1803–14. DOI: 10.1158/1541-7786.MCR-20-0359.
20. *Zhang P, Rausch C, Hastert FD, Boneva B, Filatova A, Patil SJ,* et al. Methyl-CpG binding domain protein 1 regulates localization and activity of Tet1 in a CXXC3 domain-dependent manner. Nucleic Acids Res 2017; 45(12): 7118–36. DOI: 10.1093/nar/gkx281.
21. *Liu W, Wu G, Xiong F, Chen Y*. Advances in the DNA methylation hydroxylase TET1. Biomark Res 2021; 9(1): 76. DOI: 10.1186/s40364-021-00331-7.
22. *Chen LY, Shen YA, Chu LH, Su PH, Wang HC, Weng YC,* et al. Active DNA Demethylase, TET1, Increases Oxidative Phosphorylation and Sensitizes Ovarian Cancer Stem Cells to Mitochondrial Complex I Inhibitor. Antioxidants 2024; 13(6): 735. DOI: 10.3390/antiox13060735.
23. *Ghazimoradi MH, Pakravan K, Khalafizadeh A, Babashah S*. TET1 regulates stem cell properties and cell cycle of Cancer stem cells in triple-negative breast cancer via DNA demethylation. Biochem Pharmacol 2024; 219: 115913. DOI: 10.1016/j.bcp.2023.115913.
24. *Jabbari K, Khalafizadeh A, Sheikhbahaei M, Soltaninejad H, Babashah S*. TET1: The epigenetic architect of clinical disease progression. Genes Dis 2025; 12(5): 101513. DOI: 10.1016/j.gendis.2025.101513.
25. *Zahraei M, Azimi Y, Karimipour M, Rahimi-Jamnani F, Valizadeh V, Azizi M*. CRISPR/dCas9-TET1–mediated epigenetic editing reactivates miR-200c in breast cancer cells. Sci Rep 2025; 15(1): 31739. DOI: 10.1038/s41598-025-16911-8.
26. *Xu C, Bian C, Lam R, Dong A, Min J*. The structural basis for selective binding of non-methylated CpG islands by the CFP1 CXXC domain. Nat Commun 2011; 2(1): 227. DOI: 10.1038/ncomms1237.
27. *Ceccarelli V, Valentini V, Ronchetti S, Cannarile L, Billi M, Riccardi C,* et al. Eicosapentaenoic acid induces DNA demethylation in carcinoma cells through a TET1-dependent mechanism. FASEB J 2018; fj201800245R. DOI: 10.1096/fj.201800245R.
28. *Wang Y, Hu J, Wu S, Fleishman JS, Li Y, Xu Y,* et al. Targeting epigenetic and posttranslational modifications regulating ferroptosis for the treatment of diseases. Sig Transduct Target Ther 2023; 8(1): 449. DOI: 10.1038/s41392-023-01720-0.
29. *Ouyang S, Zeng Z, He J, Luo L*. Epigenetic regulation of targeted ferroptosis: A new strategy for drug development. J Pharm Anal 2024; 14(10): 101012. DOI: 10.1016/j.jpha.2024.101012.
30. *Zhou Q, Meng Y, Le J, Sun Y, Dian Y, Yao L,* et al. Ferroptosis: mechanisms and therapeutic targets. MedComm 2024; 5(12): e70010. DOI: 10.1002/mco2.70010.
31. *Jiang X, Hu C, Ferchen K, Nie J, Cui X, Chen CH,* et al. Targeted inhibition of STAT/TET1 axis as a therapeutic strategy for acute myeloid leukemia. Nat Commun 2017; 8(1): 2099. DOI:

10.1038/s41467-017-02290-w. Erratum in: Nat Commun 2018; 9(1): 670. DOI: 10.1038/s41467-018-02947-0.

32. *Shi D, Li H, Zhang Z, He Y, Chen M, Sun L,* et al. Cryptotanshinone inhibits proliferation and induces apoptosis of breast cancer MCF-7 cells via GPER mediated PI3K/AKT signaling pathway. PLoS One 2022; 17(1): e0262389. DOI: 10.1371/journal.pone.0262389.
33. *Meng X, Yang Q, Gao Y, Liu Y, Chen F, Cao W,* et al. Longikaurin A induces ferroptosis and inhibits glioblastoma progression through DNA methylation - Mediated GPX4 suppression. Eur J Pharmacol 2024; 984: 177061. DOI: 10.1016/j.ejphar.2024.177061.

Received on July 1, 2026
Revised on August 12, 2026
Revised on August 18, 2026
Accepted on September 2, 2026
Online First November 2026